

High power impulse magnetron sputtering using a rotating cylindrical magnetron

W. P. Leroy,^{a)} S. Mahieu, and D. Depla

Department of Solid State Sciences, Ghent University, Krijgslaan 281/S1, 9000 Ghent, Belgium

A. P. Ehiasarian

Nanotechnology Center for PVD Research, Sheffield Hallam University, S1 1WB Sheffield, United Kingdom

(Received 13 July 2009; accepted 9 November 2009; published 18 December 2009)

Both the industrially favorable deposition technique, high power impulse magnetron sputtering (HIPIMS), and the industrially popular rotating cylindrical magnetron have been successfully combined. A stable operation without arcing, leaks, or other complications for the rotatable magnetron was attained, with current densities around 11 A cm^{-2} . For Ti and Al, a much higher degree in ionization in the plasma region was observed for the HIPIMS mode compared to the direct current mode. © 2010 American Vacuum Society. [DOI: 10.1116/1.3271136]

I. INTRODUCTION

Magnetron sputtering has developed immensely since its discovery and is nowadays the preferred industrial physical vapor deposition technique for a range of thin films. For large-scale industrial applications, rotating cylindrical magnetrons are becoming more and more popular than the more traditional (circular or rectangular) planar magnetrons. This success is mainly due to the better target utilization where an efficiency of 70% or more is attained, compared to approximately 30% for planar magnetrons. Because of their typical industrial size and the accompanying costs, research on these rotating cylindrical magnetrons is rare. Therefore, a small laboratory-scaled cylindrical magnetron was previously developed.¹ This allows studying the behavior of these magnetrons under well-defined conditions. Moreover, the design of the target in rotatable magnetrons allows to unveil some effects that influence the sputtering process, which would not have been considered in planar magnetron research.^{2,3}

The high power impulse magnetron sputtering (HIPIMS) as a deposition technique was first described in detail by Kouznetsov *et al.*⁴ in 1999, and has been widely discussed ever since. It proves to be a useful technique to both pretreat the substrate and to deposit high density films with excellent adhesion, high corrosion, wear resistance,^{5,6} and good optical properties.^{7,8} Therefore, HIPIMS is evolving as a favorite among deposition techniques.

Up until now, the HIPIMS technique has only been used on planar magnetrons of different sizes. In this work we report for the first time on the combination of two industrially advantageous techniques, namely, the application of HIPIMS on a rotating cylindrical magnetron.

II. EXPERIMENT

All experiments were performed in a CMS 18 vacuum system (Kurt J. Lesker) in ultrahigh vacuum conditions. The chamber was evacuated using turbomolecular pumps to a base pressure of $<10^{-4} \text{ Pa}$ (10^{-6} mbar). The working pres-

sure of Ar for the experiments was 0.4 Pa and regulated by mass flow controllers. A HIPIMS power supply (HMP2/1 Hüttinger Electronic Sp. z O.O.) was used to power the magnetron. HIPIMS of Al was operated at a frequency of 300 Hz and HIPIMS of Ti at 104 Hz. The voltage, pulse duration, and current are given in Fig. 1. To operate the magnetron in dc mode, a Hüttinger PFG1000 was used.

The plasma composition was analyzed by optical emission spectroscopy (OES) utilizing a Jobin Yvon Triax 320 scanning monochromator with resolution of 0.12 nm and a grating groove density of 1200 grooves/mm.

The ion energy distribution functions (IEDFs) and mass scans were measured using a plasma sampling energy spectrometer (PSM003, Hiden Analytical Ltd.) with a 200 μm diameter grounded orifice. The distance between the orifice and the target surface was approximately 10 cm. All mass spectrometer measurements were performed under the same working conditions of the mass spectrometer.

A next generation of the rotating cylindrical magnetron as originally described in previous work¹ has been used. The most important change to the setup was the use of a different magnet systems, which produces a higher maximal, radial magnetic field strength of 1000 G. The magnets were oriented in the direction of the mass spectrometer, in order to establish a line-of-sight measurement of the racetrack (area was $\sim 10 \text{ cm}^2$ in size). Both the Al and Ti targets were tubes with a length of 185 mm and outer diameters of 50 and 48 mm, respectively. The target rotated at a speed of 4.3 rpm.

III. RESULTS AND DISCUSSION

We believe that this is the first time HIPIMS is applied on a rotating cylindrical magnetron. Figure 1 shows the voltage and current pulses for the HIPIMS discharge of an Al and a Ti cylindrical target. These pulses are an illustration of the discharge at different voltages. Currents up to 110 A were obtained, resulting in a current density of 11 A cm^{-2} in a stable operation without (visibly) arcing, leaks, or other complications for the rotatable magnetron.

^{a)}Electronic mail: wouter.leroy@ugent.be

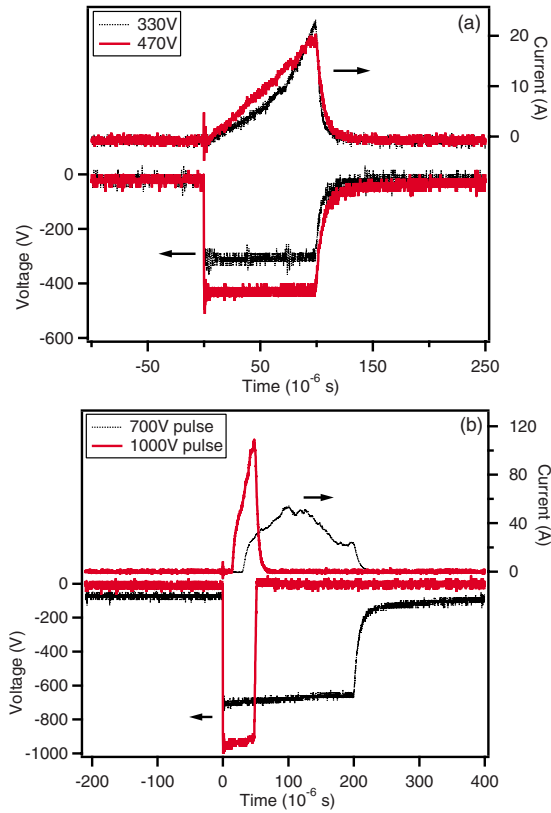


FIG. 1. (Color online) Voltage and current pulses of a HIPIMS discharge on a rotating cylindrical magnetron. Curves for an Al discharge (a) are shown, with obtained peak powers of approximately 6 and 10.8 kW. For a Ti target (b), peak powers of approximately 39 and 107 kW are obtained.

The plasma composition in dc and HIPIMS operation mode was compared. The influence of the rotation of the target on the material flux from the target was also evaluated. As shown in Fig. 2, a mass scan was performed for an Al target sputtered in normal dc, rotating HIPIMS, and stationary HIPIMS mode. One can see a clear difference between the dc and the HIPIMS modes, where the latter results in an increase in both Ar ions, as well as Al ions. The number increased approximately by a factor of 150 for Al^{1+} ions, 50 for Al^{2+} ions, 10 for Ar^{1+} ions, and by a factor of 3 for Ar^{2+}

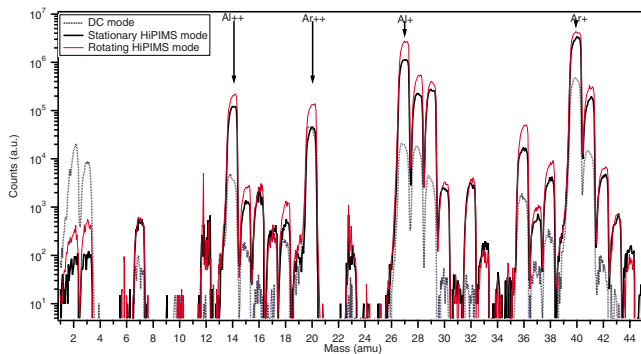


FIG. 2. (Color online) Mass scan of a cylindrical Al target sputtered in dc mode (dotted line), stationary HIPIMS mode (full thick line), and rotating HIPIMS mode (full thin line).

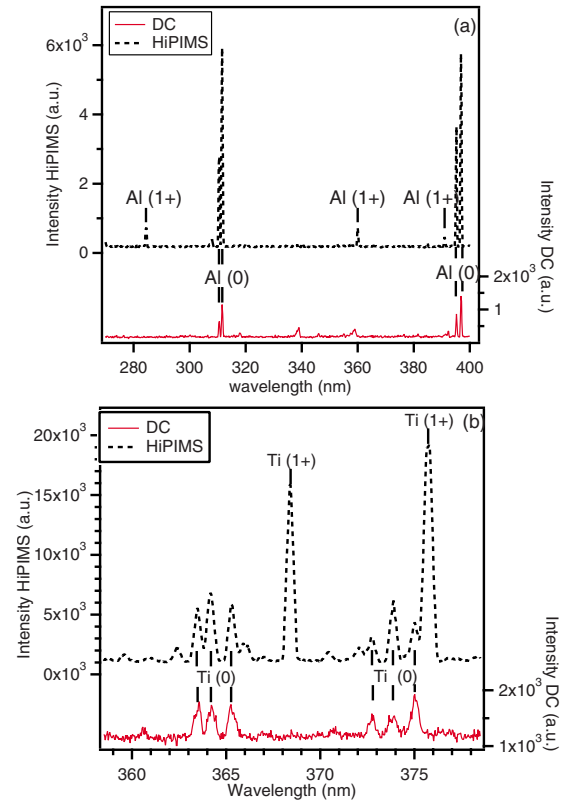


FIG. 3. (Color online) OES spectra of a dc and a HIPIMS discharge from a rotating cylindrical magnetron with an Al (a) or a Ti (b) target.

ions. Thus a significant increase in metal content in the HIPIMS plasma was detected compared to dc. Furthermore, there seems to be only a small difference between the rotating and stationary HIPIMS modes. The difference in operation is only the rotation of the target. Therefore, the slightly higher ion intensity is probably due to a better cooling of the target surface or due to the redeposition effect,² when sputtering in a rotating mode. Nevertheless, this difference is small so only the rotating mode will be discussed further in this manuscript.

Figure 3 shows the OES spectra of both dc and HIPIMS plasmas for the Al and Ti targets. In both cases it can clearly be seen that we get a higher degree of ionization of the metallic particles. The emission intensity is proportional to the product of the oscillator strength of the particular transition and the density of the excited species.⁹ However, it also depends on the excitation energy of the level and the energy and density of excitation species—in this case, electrons.^{10,11} An approximation of the density can be extracted from the measured emission intensity and tabulated oscillator strengths. The effect of electron temperature can be neglected since electron temperatures are relatively low, <2 eV, and depend weakly on the target material according to literature published for Cr and Ti.¹² Calculations, neglecting electron temperature are given in Table I.

To obtain the relative concentration, the average density for ions and neutrals was obtained from the different states.

TABLE I. Approximation of the density, extracted from the measured emission intensity and tabulated oscillator strengths for Al and Ti in HIPIMS.

Metal species	Wavelength (nm)	Oscillator strength	Excitation energy (eV)	Intensity (arb.u.)	Approximate density (arb.u.)	Relative concentration
Al (0)	394.40	0.11	3.15	3450	30	10% \pm 5%
Al (0)	396.15	0.229	3.15	5550	25	
Al (1+)	390.06	0.001 09	10.6	250	230	90% \pm 10%
Ti (0)	363.54	0.181	3.41	5.1	28	25% \pm 8%
Ti (0)	364.27	0.175	3.43	6.7	38	
Ti (0)	365.35	0.172	3.45	5.7	33	
Ti (1+)	368.52	0.149	3.98	16	107	75% \pm 10%
Ti (1+)	375.93	0.233	3.91	19	81	

In this procedure we selected lines that are close in wavelength which allows neglecting corrections due to the spectral sensitivity of the spectrometer.

Since the excitation energy for Al(1+) 390.06 nm is four times higher than the energy for Al(0) 394.40 and 396.15 nm, we expect a significantly lower number of electrons with sufficient energy to create the excitation. Thus, in terms of Table I, the levels for neutrals are excited at much higher rate than the levels of ions and we can assume that the density quoted in the table is underestimated. The ionization degree in the dense plasma region is of the order of 90%. This rough estimation fits well with measurements on HIPIMS of Ti on planar cathodes.¹³ It is expected that near the substrate ionization degree would be lower due to the preferential trapping of metal ions by the magnetic and electric fields of the magnetron.

In the case of HIPIMS of Ti, the ion and neutral excitations have similar energy of 3.9 and 3.4 eV, respectively. The lines appear close to each other and there was no strong variation in sensitivity of the spectrometer. Therefore the measured emission intensity and oscillator strengths are good indicators of density. On this basis, the ionization fraction in the dense plasma region can be estimated to be of the order of 75%.

In both Ti and Al ionization, we assume that the creation of ion excited states requires at least two collisions: one to ionize the neutral atom and a second to excite the resulting ion. This is consistent with models of the magnetron¹⁴ and HIPIMS.¹⁰

To get a better quantitative idea about the metal ionization degree, we performed IEDF scans on the rotating cylindrical Ti target in dc and HIPIMS mode. The IEDFs ranged from -20 up to 100 eV and Fig. 4(a) shows the integrated amounts for each of the ion types. It can clearly be seen that there is a higher degree in ionization for the HIPIMS mode, especially for the metal ionization.

Furthermore the ratio of the metal ions to the argon ions as a function of power [see Fig. 4(b)] has a clear trend of increasing metal ionization, which is typical for HIPIMS discharges. For the higher peak powers, the ratio of doubly

charged ions $\text{Ti}^{2+}/\text{Ar}^{2+}$ is greater than for the Ti^+/Ar^+ ratio. This is due to a big increase in the amount of Ti^{2+} ions, while the amount of Ar^{2+} remains quite constant.

IV. CONCLUSION

We report for the first time the successful combination of two industrially favorable techniques: HIPIMS and a rotating cylindrical magnetron. High peak currents are attained without any problem for Al and Ti targets. Furthermore it was shown that the HIPIMS plasma consists in a high degree of ionized metal particles. We think this combination of techniques can be a great tool for industrial applications, as the

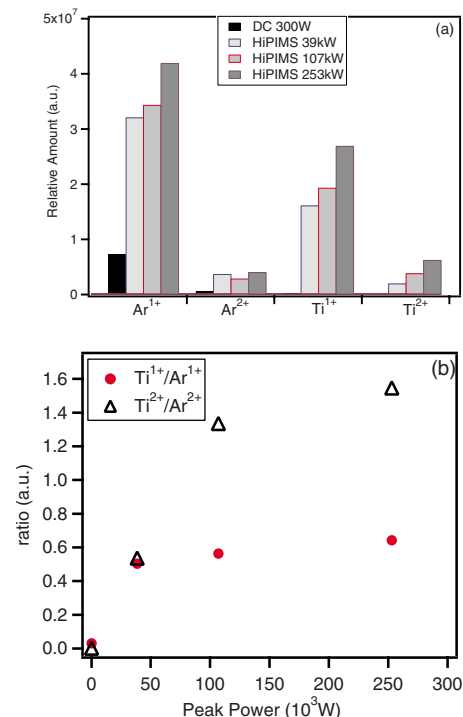


FIG. 4. (Color online) Integrated amount of ions from the IEDF for a rotating cylindrical magnetron with a Ti target.

advantages of both techniques (high degree of metal ionization and very efficient target consumption) can be fully exploited.

ACKNOWLEDGMENTS

This work was partially funded by the Institute for the Promotion of Innovation through Science and Technology in Flanders (IWT-Vlaanderen), under SBO Project No. 60030. One of the authors (S.M.) acknowledges the Research Foundation of Flanders (FWO-Flanders) for financial support. A.E. acknowledges the support of the EPSRC in U.K. under Grant No. EP/D049202/1.

¹D. Depla, J. Haemers, G. Buyle, and R. De Gryse, *J. Vac. Sci. Technol. A* **24**, 934 (2006).

²X. Y. Li, D. Depla, W. P. Leroy, J. Haemers, and R. De Gryse, *J. Phys. D: Appl. Phys.* **41**, 035203 (2008).

³S. Mahieu, W. P. Leroy, D. Depla, S. Schreiber, and W. Moller, *Appl.*

Phys. Lett. **93**, 061501 (2008).

⁴V. Kouznetsov, K. Macak, J. M. Schneider, U. Helmersson, and I. Petrov, *Surf. Coat. Technol.* **122**, 290 (1999).

⁵A. P. Ehasarian, J. G. Wen, and I. Petrov, *J. Appl. Phys.* **101**, 054301 (2007).

⁶Y. P. Purandare, A. P. Ehasarian, and P. E. Hovsepian, *J. Vac. Sci. Technol. A* **26**, 288 (2008).

⁷S. Konstantinidis, J. P. Dauchot, and A. Hecq, *33rd International Conference on Metallurgical Coatings and Thin Films*, San Diego, CA (Elsevier Science, New York, 2006); *Thin Solid Films* **515**, 1182 (2006).

⁸S. Konstantinidis, A. Hemberg, J. P. Dauchot, and M. Hecq, *J. Vac. Sci. Technol. B* **25**, L19 (2007).

⁹J. W. Bradley and T. Welzel, in *Reactive Sputter Deposition*, edited by D. Depla and S. Mahieu (Springer-Verlag, Berlin, 2008), p. 255.

¹⁰A. P. Ehasarian, A. Vetushka, A. Hecimovic, and S. Konstantinidis, *J. Appl. Phys.* **104**, 083305 (2008).

¹¹C. Christou and Z. H. Barber, *J. Vac. Sci. Technol. A* **18**, 2897 (2000).

¹²A. Vetushka and A. P. Ehasarian, *J. Phys. D: Appl. Phys.* **41**, 015204 (2008).

¹³J. Bohlmark, J. Alami, C. Christou, A. P. Ehasarian, and U. Helmersson, *J. Vac. Sci. Technol. A* **23**, 18 (2005).

¹⁴S. M. Rossnagel and K. L. Saenger, *J. Vac. Sci. Technol. A* **7**, 968 (1989).

Copyright of Journal of Vacuum Science & Technology: Part A is the property of AVS, The Science & Technology Society and its content may not be copied or emailed to multiple sites or posted to a listserv without the copyright holder's express written permission. However, users may print, download, or email articles for individual use.